EXPERIMENTAL AND NUMERICAL STUDY OF F-T/BIODIESEL/BIOETHANOL SURROGATE FUEL OXIDATION IN JET-STIRRED REACTOR

May-Carle J.-B.[a,b,*], Pidol L.[a], Nicolle A.[a], Anderlohr J.[a], Togbé C.[b], and Dagaut P.[b]
*jean-baptiste.may-carle@ifpen.fr
[a]IFP Energies Nouvelles, 1 & 4 avenue de Bois-Préau, 92500 Rueil-Malmaison, France
[b]CNRS-INSIS, 1C, Avenue de la Recherche Scientifique, 45071 Orléans Cedex 2, France

Abstract
There is growing interest for using alternative fuels in compression ignition (CI) engines. Among them, blends of Fischer-Tropsch (F-T), biodiesel, and ethanol seem to be a promising fuel for diesel engine applications. An advanced control of current diesel engines requires a detailed comprehension of the fuel chemistry in terms of auto-ignition and pollutant formation. Such understanding is generally obtained by experimental studies performed on fuel oxidation or by kinetic modeling. However, neither experimental data, nor convenient combustion models were available for such an alternative fuel. Therefore, the kinetics of oxidation of F-T, F-T/biodiesel and F-T/biodiesel/bioethanol surrogate fuel (n-decane, iso-octane, methyl octanoate, and ethanol) were studied experimentally in a jet-stirred reactor (JSR) at 10 atm and constant residence time of 1 s, over the temperature range of 560-1160 K, and for several equivalence ratios (0.5-2). Concentration profiles of reactants, stable intermediates and final products were obtained by probe sampling followed by online Fourier transformed infrared spectroscopy (FTIR) and off-line gas chromatography analyses. The oxidation of these fuels was modeled using a detailed chemical kinetic reaction mechanism consisting of 9919 reactions and 2202 species. The proposed kinetic reaction mechanism yields a good representation of the kinetics of oxidation of the tested biofuel blends.

1. Introduction
The use of renewable fuel is a promising way to reduce the dependence on fossil fuels petroleum and to minimize the green-house gases emissions. Today, mixtures of monoalkyl esters of long carbon-chain fatty acid (a.k.a. biodiesel) are mixed in variable quantities with current diesel fuels [1,2]. These alkyl esters are obtained from transesterification of renewable lipid feedstock (mostly vegetable but eventually from animal fat and waste) with methanol or ethanol [3,4]. Reduced emissions of soot have been reported, indicating biodiesel may be useful for preserving our environment [5].

Ethanol is an attractive renewable fuel due to its availability in large volume, especially with the second generation process that will be available in the near future [6]. It is mostly used in spark ignition (SI) engines, whereas its use in diesel engines is difficult because of its low cetane number [1,7]. Nevertheless, there is a growing proportion of diesel car in Europe, together with a shortage in diesel fuel production and an overproduction of gasoline. Therefore, using ethanol in diesel engines would be helpful to balance the diesel fuel/gasoline consumption. Furthermore, ethanol provides a strong potential to reduce particulate emissions in compression-ignition (CI) engines [8-10]. However, the solubility of ethanol in petrol-derived diesel is rather limited [11]. In order to solve this issue, biodiesel may be used as a cosolvent for increasing ethanol solubility in diesel fuels and preventing phase separation [12-21]. Unfortunately, ethanol addition also decreases the cetane number of the blend [7,22]. This may lead to misfiring diesel engines under some conditions. In order to avoid this issue,

fossil diesel fuel could be replaced by Fischer-Tropsch diesel fuel (F-T) having convenient auto-ignition properties [23,24]. F-T fuel is a synthetic fuel manufactured via Fischer-Tropsch conversion of syngas yielding liquid straight-chain paraffins, and alternatively, after further processing, branched paraffins and cyclic hydrocarbon mixtures. The raw material can either be natural gas (the final liquid fuel being called GtL), coal (CtL) or residual biomass (BtL). The high cetane number of such fuels can make up for the low auto-ignition properties of ethanol. That is why, F-T/biodiesel/bioethanol mixtures show a very high potential for diesel engine applications. In the future, when BtL will be available, BtL/biodiesel/bioethanol blends would be very interesting as 100% biofuel blends. However, nowadays, there is a great lack of experimental and kinetic data for the combustion of such blends. This paper is a first step towards understanding the oxidation of F-T/biodiesel/bioethanol.

Conventional fuels consist of complex mixtures of thousand of high molecular weight hydrocarbons involving thousands of chemical reactions. Therefore, surrogates are employed to represent fuel with a limited number of components, allowing a molecular level understanding of fuel oxidation processes. F-T diesel fuels are complex mixtures of n-alkane and iso-alkane compounds from C_8 to C_{24}. In a previous study, a surrogate mixture of n-decane and iso-octane was used satisfactorily to represent the oxidation of a F-T jet fuel [25]. Thus, in the present study, a blend of 68% n-decane/32% iso-octane (in mole) was chosen to represent a F-T diesel fuel. This blend has a H/C ratio and cetane number close to those of F-T diesel fuel. Rapeseed oil methyl esters (RME), mostly used as biodiesel in Europe, consist mainly of C_{18} esters with highly saturated carbon chains. A blend of n-decane and methyl octanoate was previously used as a surrogate for biodiesel oxidation [26]. Thus, in the present study, a 50% methyl octanoate/50% n-decane (in mole) mixture is proposed to represent RME oxidation. This blend has properties similar to those of biodiesel: a very close empirical formula (with same C/O ratio of 9,5), a density of 835 $kg.m^{-3}$ and a similar affinity to auto-ignition.

In this paper, we present new experimental results obtained in a jet stirred reactor (JSR) at 10 atm for the oxidation of n-decane, iso-octane, methyl octanoate and ethanol mixtures over a wide range of equivalence ratios (0.5 to 2) and temperatures (560-1160 K). The oxidation of the chosen F-T/biodiesel/bioethanol surrogate was modeled using a detailed kinetic reaction mechanism consisting of 2202 species and 9919 reactions.

2. Experimental setup

The JSR used here is similar to that already described by Dagaut et al. [27]. It consists of a small sphere of 4 cm diameter (39 cm^3) made of fused-silica (to minimize wall catalytic reactions), equipped with 4 nozzles of 1 mm diameter for the admission of the gases achieving the stirring. The liquid fuel mixtures were atomized and vaporized before injection into the reactor. All the gases were preheated to minimize temperature gradients inside the JSR. Good thermal homogeneity along the vertical axis of the reactor was observed for each experiment by thermocouples (0.1 mm Pt-Pt/Rh 10% located inside a thin-wall silica tube). The experiments were performed at steady state, at a constant mean residence time of 1 s, with the reactants continually flowing into the reactor, whereas the temperature inside the JSR was varied stepwise. A high degree of dilution was used, reducing temperature gradients and heat release in the JSR. Under these conditions, no flame occurred in the JSR. The reacting mixtures were sampled by means of a fused-silica low pressure sonic probe. The samples (4-6 kPa) were taken at steady temperature and residence time. They were analyzed off-line by gas chromatography-mass spectroscopy (GC-MS) after collection and storage in 1 L Pyrex bulbs. Online FTIR analyses (Nicolet Nexus; 0.5 cm^{-1} resolution) of the reacting gases were also performed by connecting the sampling probe to a temperature control (140°C) gas cell (10m path length) via a Teflon heated line (210°C). This analytical equipment allowed measuring

the concentrations of H_2O, CO, CO_2, CH_2O, CH_4, C_2H_2 and C_2H_4. Gas chromatographs equipped with capillary columns (DB-5 ms, DB-624, Plot Al_2O_3/KCl and carboplot-P7), a thermal conductivity detector (TCD) and a flame ionization detector (FID) were used for species measurements. Compounds identification was made via GC-MS analyses using a quadrupole (V1200, Varian) operating in electron impact ionization mode (70 eV). A good repeatability of the measurement and a reasonably good carbon balance (100 ± 10%) were obtained in this series of experiment.

In this paper, the oxidation of 3 blends was studied at 10 atm in a JSR, over the temperature range of 560-1160 K and at a mean residence time of 1 s. This temperature range allowed to study the low temperature oxidation regime, the negative temperature coefficient (NTC) regime and the high temperature oxidation regime. The experiments were performed at three equivalence ratios (ϕ = 0.5, 1, and 2). The initial reactant mole fractions are reported in Table1. The A mixture is a blend of n-decane and iso-octane representative of a F-T diesel fuel. B mixture is used to simulate the oxidation behavior of a blend containing 40 % F-T and 60 % RME (in volume). C mixture represents F-T/RME/bioethanol blend containing 10 % ethanol (in volume). In this blend, the volume of biodiesel and ethanol is equal in order to avoid solubility issues. B and C mixtures have been chosen since they have close C/O ratios.

Table 1. Oxidation of surrogate fuel mixtures in a JSR at 10 atm and 1s: experimental conditions

Mixtures	Reference fuel composition (volume %)	Initial mole fractions (ppm)			
		$c_{10}h_{22}$	Ic_8h_{18}	$c_9h_{18}o_2$	c_2h_5oh
A	F-T	1020	470	/	/
B	F-T40/RME60	573	127	300	/
C	F-T80/RME10/EtOH10	491	207	41	261

More than 30 species were identified and measured by GC-MS and FID. Thus, experimental concentration profiles were obtained for H_2, O_2, H_2O, CO, CO_2, methanal (CH_2O), ethanal (CH_3HCO), propanal (C_2H_5HCO), acrolein (C_2H_3HCO), butanal (C_3H_7HCO), pentanal (C_4H_9HCO), hexanal ($C_5H_{11}HCO$), acetone (CH_3COCH_3), methanol (CH_3OH), methane (CH_4), ethane (C_2H_6), ethene (C_2H_4), acetylene (C_2H_2), propene (C_3H_6), butene (C_4H_8), 1,3-butadiene (1,3-C_4H_6), 1-pentene (1-C_5H_{10}), 1-hexene (1-C_6H_{12}), 1-heptene (1-C_7H_{14}), benzene (C_6H_6), oxirane (C_2H_4O), methyl 2-propenoate, n-decane ($C_{10}H_{22}$), iso-octane (IC_8H_{18}), methyl octanoate ($C_9H_{18}O_2$) and ethanol (C_2H_5OH). A good repeatability of the result was observed. The accuracy of the mole fractions was typically ±10%, whereas the uncertainty on the experimental temperature was ±8K. Other minor species detected at part per million (ppm) levels were neither quantified nor used in the modeling.

3. Kinetic modeling

The kinetic modeling was performed using the Chemkin package [28,29]. The JSR computations were performed using the PSR code [30] which allows to compute species concentrations from the balance between the net rate of production of each species by chemical reactions and the difference between the input and output species flow rates. These rates are computed from the kinetic reaction mechanism and the rate constant of the elementary reactions calculated at the experimental temperature, using the modified Arrhenius equation:

$$k = A\,T^{n}\,\exp\left(\frac{-E}{RT}\right) \qquad (1)$$

The detailed chemical kinetic mechanism used here is based on previous studies of the oxidation of n-decane [31], iso-octane [32], methyl octanoate [33] and ethanol [34]. The kinetic oxidation of each hydrocarbon has been developed separately and merged to simulate the oxidation of F-T/biodiesel/ethanol blends. The proposed kinetic reaction mechanism consisting of 9919 reversible reactions involving 2202 species is available from the authors.

4. Results and discussion

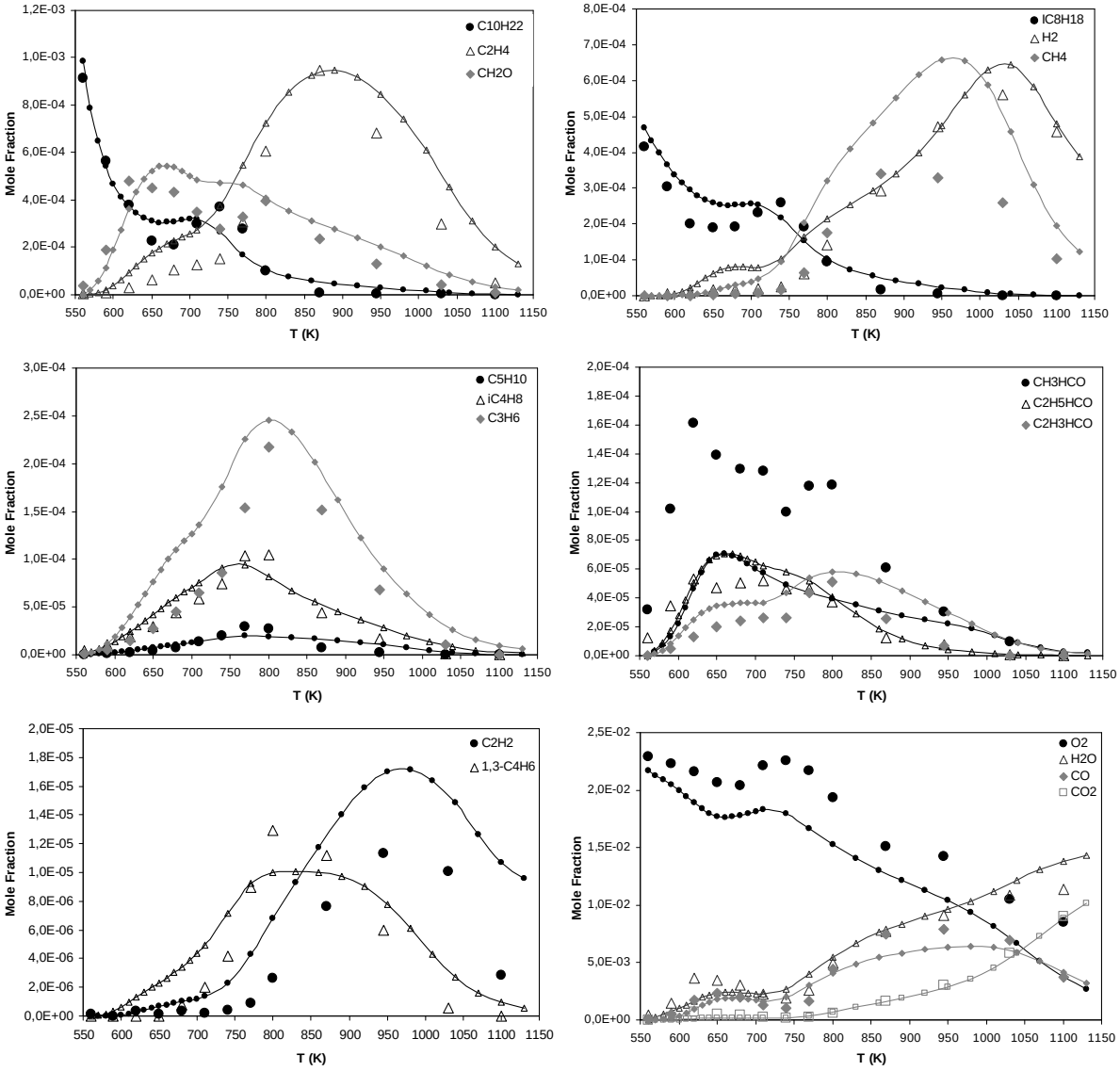

Figure 1. Oxidation of mixture A in a JSR (ϕ=1, O_2=21774 ppm, P=10 atm). Experimental data (large symbols) are compared to computational results (lines and small symbols).

The obtained new set of experimental data was used to validate the detailed chemical kinetic reaction mechanism mentioned above for the oxidation of n-decane/iso-octane/methyl octanoate/ethanol blends. Comparisons between experimental and computational results are presented in Figures 1-5. Figures 1-3 show the oxidation of the different blends at stoechiometry ($\phi = 1$), while Figures 4 and 5 present results obtained for variation of the equivalence ratio ($\phi = 0.5$ and 2) during the oxidation of mixture C. As can be seen from these Figures, the proposed model represents fairly well the oxidation kinetics of the tested

mixtures. The mole fractions of most of the stable intermediates were also well predicted by the model.

4.1 Impact of biodiesel

The present data set was used to study the impact of the initial experimental conditions on the formation of intermediate products. Figures 1 and 2 show the species profiles obtained for the oxidation of fuel surrogates A and B. Unsatured methyl esters, such as methyl prop-2-enoate, were formed by oxidation of methyl octanoate. However, the amount of methyl octanoate is very low in most of the blends (cf. table 1), and thus methyl esters are produced in such low amounts that these species could not always be detected. We observed as well that increasing the amount of biodiesel in the blend enhances ethylene emissions. For example, at $\phi = 1$, the maximum normalized mole fraction of ethylene (i.e. 100*[maximum experimental mole fraction/initial total carbon mole fraction]) was 6.97 for the A mixture and 8.15 for the B mixture.

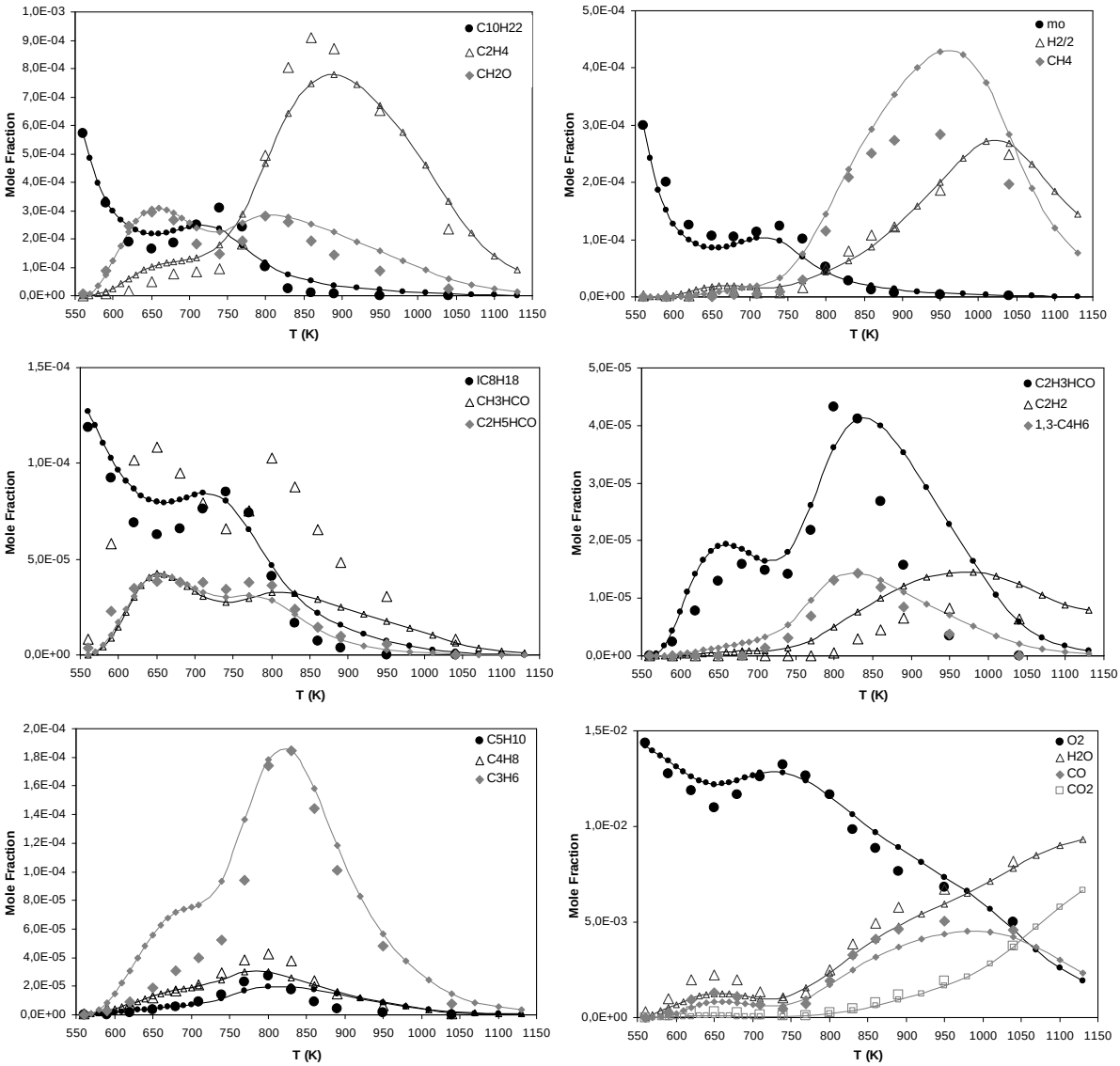

Figure 2. Oxidation of mixture B in a JSR (ϕ=1, O_2=14220 ppm, P=10 atm). Experimental data (large symbols) are compared to computational results (lines and small symbols).

4.2 Impact of ethanol

Figure 3 shows the species profiles obtained for the oxidation of mixture C at ϕ=1. One interesting feature of the oxidation of this blend is that ethanol is oxidized under the low-temperature regime (550-750 K) whereas, under similar conditions, no oxidation of ethanol would occur if it was the only fuel injected, in agreement with recent flow-reactor studies [35]. Indeed, the oxidation of the most reactive fuel (i.e. n-decane and methyl octanoate) produces radicals which can initiate the oxidation of the ethanol.

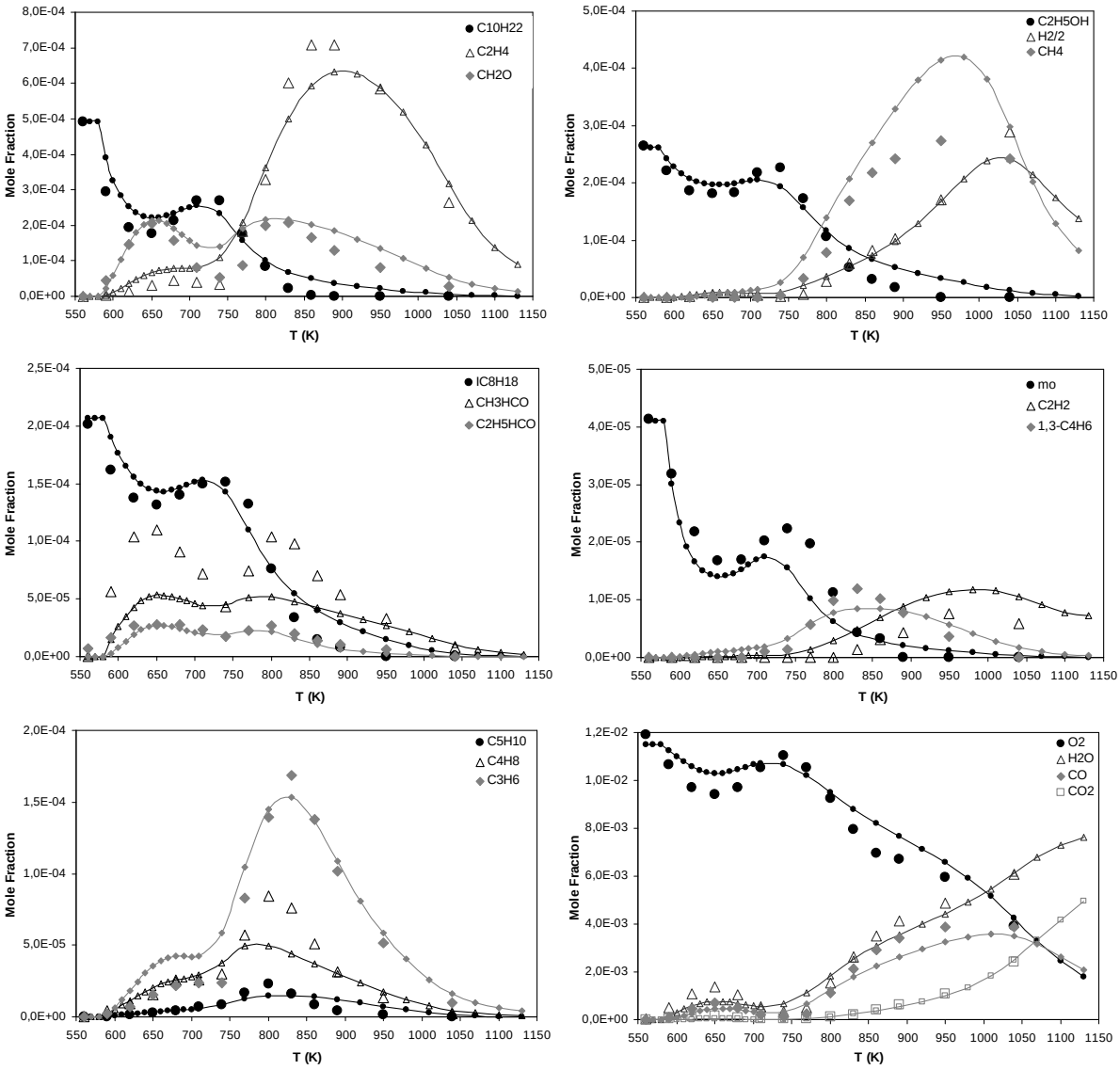

Figure 3. Oxidation of mixture C in a JSR (ϕ=1, O_2=11498 ppm, P=10 atm). Experimental data (large symbols) are compared to computational results (lines and small symbols).

The data also indicates that the introduction of ethanol in the blend results in higher maximum mole fraction of acetaldehyde. As can be seen from Figures 1, 2 and 3, at ϕ = 1, the maximum normalized mole fraction of acetaldehyde was 1.15 for the mixture A, 1,14 for the mixture B and 1.47 for the mixture C. Actually, this result confirms engine data showing increased emissions of acetaldehyde with ethanol/diesel fuel mixtures and raise some concerns regarding the impact on air quality of an extensive use of ethanol in CI engines [20,21,36-38].

4.3 Impact of equivalence ratio

In this study, the equivalence ratio was varied from 0.5 to 2. By comparing Figures 4-6, we observed that a higher initial concentration of oxygen in the reacting mixture leads to an increase of the fuel conversion. We noticed that decreasing the initial oxygen concentration resulted in higher maximum concentrations of intermediates. In the mixture C, the ethylene maximum normalized mole fraction varied from 5.72 at $\phi = 0.5$ (Figure 5) to 11.6 at $\phi = 2$ (Figure 6). These variations resulted from the reduction of the radical pool with a decreasing oxygen initial concentration.

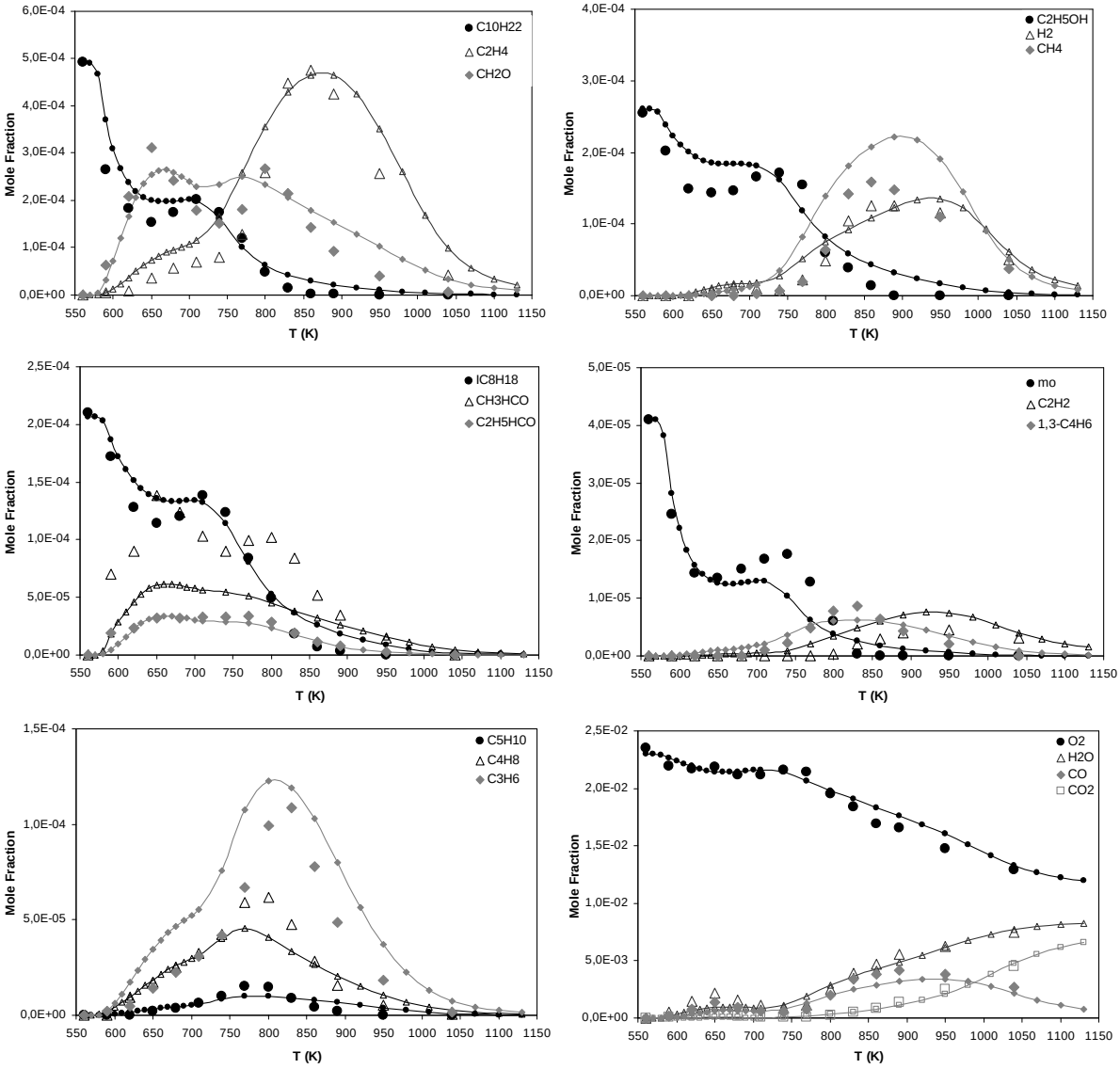

Figure 4. Oxidation of mixture C in a JSR (ϕ=0.5, O_2=22995 ppm, P=10 atm). Experimental data (large symbols) are compared to computational results (lines and small symbols).

The model predicts fairly well the experimentally observed overall reactivity of the different blends. However, it tends to underestimate the overall rate of oxidation below 750K for the mixtures containing a large amount of ethanol. This behavior could result from a too strong inhibiting effect of ethanol on fuel oxidation that could be due to missing cross reactions for n-decane and ethanol. The mole fractions of most of the stable intermediates were also well predicted by the model. Nevertheless, it should be noticed that the model over predicts the maximum mole fractions of methane. That could indicate that the kinetics of

methyl radicals should be revised, and particularly the ratio between recombination to form ethane and oxidation route. It is also noticed that the model tends to under predict the formation of acetaldehyde.

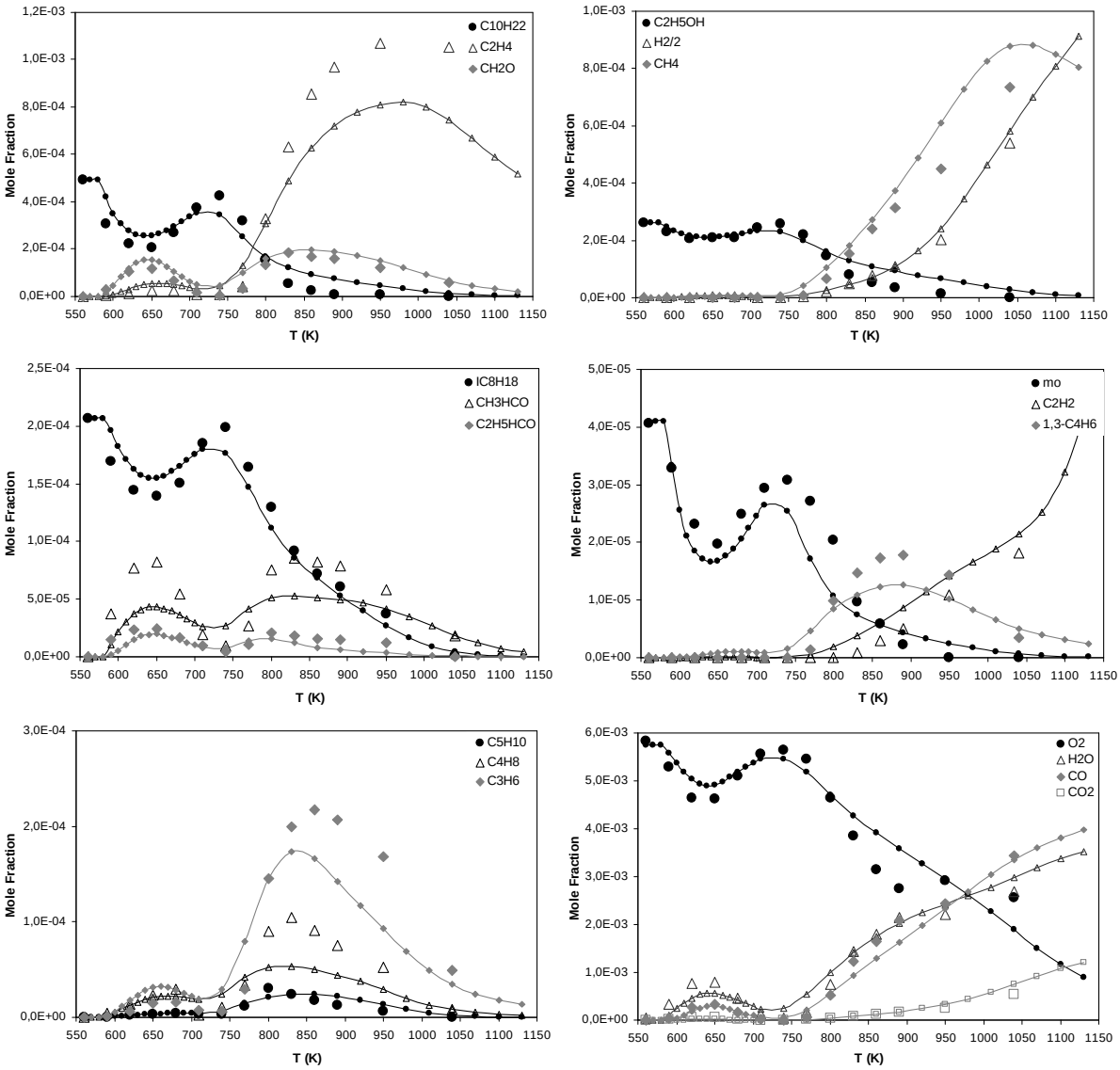

Figure 5. Oxidation of mixture C in a JSR (ϕ=2, O_2=5749 ppm, P=10 atm). Experimental data (large symbols) are compared to the computational results (lines and small symbols).

4.4 Comparison of obtained results

Figure 6 shows the oxidation of n-decane for 3 mixtures at 3 equivalence ratio. N-decane is the most reactive component of the different fuel blends. It thus governs the global reactivity and is a key species in all tested fuel blends

As can be seen from Figure 6, the introduction of biodiesel in the blend has no strong impact on fuel reactivity, despite the high amount of biodiesel (60% vol.) in mixture B. Indeed, reactivity of n-decane for mixtures A and B is quite similar as methyl octanoate and n-decane have similar reactivity.

On the other hand, increasing the amount of ethanol in the blend has a strong impact on global reactivity of the fuel. Compared to mixture A, the oxidation of mixture C is inhibited under all conditions between 600 and 850 K. At ϕ=0.5, the n-decane profiles of mixture C are shifted towards higher concentrations over the complete temperature range

between 600 and 850 K. A slight increase of the NTC-amplitude between 650 and 750 K is observed as well. When compared to mixture A, the oxidation of mixture C is considerably inhibited up to 800 K. Under stoichiometric conditions ($\phi = 1$) a slight increase of the NTC-amplitude is observed. However, at temperatures above 750 K, the oxidation of mixture C is less inhibited. Under rich conditions ($\phi = 2$) the presence of ethanol results in a strong increase of the NTC amplitude between 650 and 750K, where at 650 K and 800 K the reactivity of mixtures A and C is almost the same. The strong impact of ethanol in the NTC-temperature range under rich conditions will be investigated in the following by a reaction path analysis.

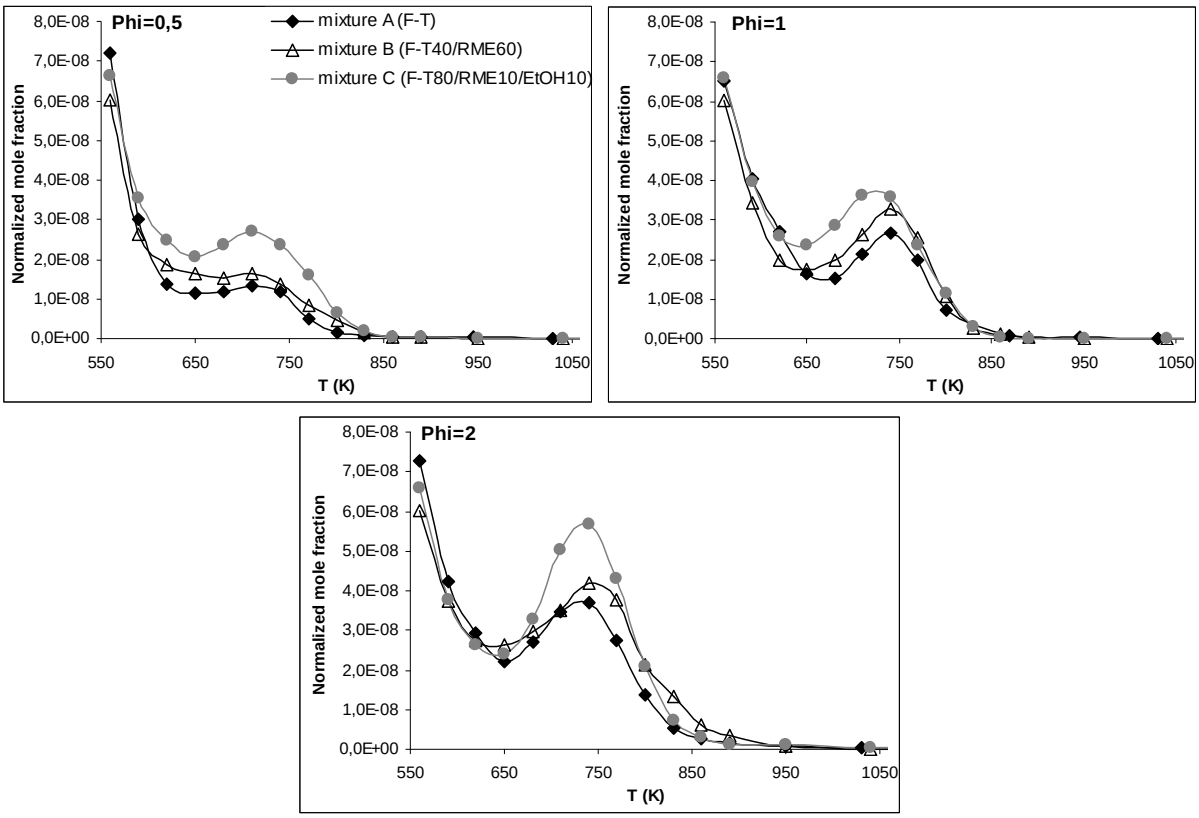

Figure 6. Normalized mole fractions of n-decane during the oxidation of mixture A, B and C in a JSR

4.5 Reaction paths analysis

In order to investigate the impact of ethanol on the NTC-amplitude under rich conditions, a kinetic reaction path analysis was performed for the oxidation of mixtures A and C at a pressure of 10 atm, $\phi = 2$ and at a temperature of 740 K, where the inhibiting effect of ethanol on n-decane oxidation is maximum (see Figure 6). Table 2 presents net rate of production (ROP in mol.cm^{-3}.s) and normalized rate of production (NROP) for some key species, at 740 K, for blends A and C. Normalized rates of production have been determined by dividing the rate of production of each species to the rate of consumption of n-decane (respectively 1.05×10^{-7} mol.cm^{-3}.s for mixture A and 2.42×10^{-8} mol.cm^{-3}.s for mixture C).

Table 2 shows that the formation of alkyl radicals (R) and the addition of oxygen molecules to give peroxy radicals (ROO) are quite similar for blends A and C. However, the presence of ethanol strongly promotes the decomposition of hydroperoxyalkyl radicals (QOOH) into ketones or cyclic ether. When ethanol is present, 41.9% of OH radicals are produced by QOOH decomposition, while for mixture A only 16.1% of OH radicals are produced by the same reaction path.

Table 2. Flow analysis for rich oxidation of A and C mixtures in PSR at a pressure of 10 atm and a temperature of 740 K

		Mixture A		Mixture C	
Species	Reactions	ROP ($mol.cm^{-3}.s$)	NROP (%)	ROP ($mol.cm^{-3}.s$)	NROP (%)
R	$RH+OH=R+H_2O$	$9.64x10^{-8}$	**91.8**	$2.21x10^{-8}$	**91.3**
ROO	$R+O_2=ROO$	$8.10x10^{-8}$	**77.2**	$1.77x10^{-8}$	**73.2**
CH3	$CH_3CO+M=CH_3+CO+M$	$3.50x10^{-8}$	**33.3**	$3.08x10^{-9}$	**12.7**
HCO	$CH_2O+OH=HCO+H_2O$	$3.91x10^{-8}$	**37.2**	$1.38x10^{-9}$	**5.7**
	$C_2H_3+O_2=CH_2O+HCO$	$1.17x10^{-8}$	**11.1**	$5.88x10^{-10}$	**2.4**
OH	QOOH=OH+products	$1.69x10^{-8}$	**16.1**	$1.01x10^{-8}$	**41.9**
	$H_2O_2+M=OH+OH+M$	$6.91x10^{-8}$	**65.8**	$9.71x10^{-9}$	**40.1**
HO_2	$HCO+O_2=CO+HO_2$	$6.91x10^{-8}$	**65.8**	$2.82x10^{-9}$	**11.7**
	$C_2H_4O_2H=C_2H_4+HO_2$	$2.51x10^{-8}$	**23.9**	$2.67x10^{-9}$	**11.0**
	$H+O_2+M=HO_2+M$	$2.30x10^{-8}$	**21.9**	$2.38x10^{-9}$	**9.8**
	$CH_3CHOH+O_2=CH_3HCO+HO_2$	0	**0**	$4.27x10^{-9}$	**17.7**
	$R+O_2=alkene+HO_2$	0	**0**	$3.43x10^{-9}$	**14.2**

QOOH decomposition is a chain propagating reaction step and competes with the addition of oxygen to QOOH, which finally leads into a chain branching decomposition of hydroperoxyalkylperoxy radicals (OOQOOH). Consequently, in the mixture C, the chain branching decomposition of OOQOOH radicals is disfavored and leads to a slower production of radicals. This explains the observed inhibiting impact of ethanol on n-decane under the examined conditions. The resulting increased concentrations of OH radicals within mixture A leads to an increased production of oxidation intermediates such as methyl radicals (CH_3) and HCO. It is important to notice that the higher concentration of HO_2 is not due to the oxidation of alkyl radicals, but to favored oxidation of HCO to CO.

5. Conclusion

The oxidation of n-decane/iso-octane/methyl octanoate/ethanol blends was studied experimentally in a jet stirred reactor at 10 atm and constant residence time of 1 s, over the temperature range 560-1160 K, and for equivalence ratios in the range 0.5-2. The concentration profiles of reactants, stable intermediates and final products were measured by sonic probe sampling followed by on-line FTIR analysis and off-line GC analyses.

The kinetics of oxidation of these blends were modeled from low to high temperature, using a detailed chemical kinetic reaction mechanism consisting of 2202 species and 9919 reversible reactions. The kinetic modeling gave an overall good representation of the experimental results. The reaction mechanism was also used to identify the governing reaction paths involved in the oxidation of a chosen surrogate F-T/biodiesel/bioethanol blend. Further validation of this kinetic scheme over different experimental devices would be helpful to reach a better understanding of the combustion of such a biofuel.

A strong inhibiting effect of ethanol on the NTC oxidation regime under rich conditions have been observed experimentally, and investigated by a reaction path analysis. It would be interesting to vary the amount of ethanol in the blend in order to fully understand the impact of ethanol on fuel reactivity.

Acknowledgements. The authors thank Drs. Pascal Diévart, Guillaume Dayma, Anne Jaecker and Nicolas Jeuland for their interest in this work and their assistance.

References

[1] Agarwal A.K., "Biofuels (alcohols and biodiesel) applications as fuels for internal combustion engines", *Progress in Energy and Combustion Science* 33:233-271 (2007).
[2] Shahid E.M., Jamal Y., "A review of biodiesel as vehicular fuel", *Renewable and Sustainable Energy Reviews* 12:2484-2494 (2008).
[3] Demirbas A., "Progress and recent trends in biodiesel fuels", *Energy Conversion and Management* 50:14-34 (2009).
[4] Murugesan A., Umarani C., Chinnusamy T.R., Krishnan M., Subramanian R., Neduzchezhain N., "Production and analysis of bio-diesel from non-edible oils - a review", *Renewable and Sustainable Energy Reviews* 13:825-834 (2009).
[5] Lapuerta M., Armas O., Rodrigez-Fernandez J., "Effect of biodiesel fuels on diesel engine emissions", *Progress in Energy and Combustion Science* 34:198-223 (2008).
[6] Balat M., Balat H., Öz C., "Progress in bioethanol processing", *Progress in Energy and Combustion Science* 34:551-573 (2008).
[7] Hansen A.C., Zhang Q., Lyne P.W.L., "Ethanol-diesel fuel blends: a review", *Bioresource Technology* 96:277-285 (2005).
[8] Chen H., Wang J., Shuai S., Wenmiao C., "Study of oxygenated biomass fuel blends on a diesel engine", *Fuel* 87:3462-3468 (2008).
[9] Lapuerta M., Armas O., Herreros J.M., "Emissions from a diesel-bioethanol blend in an automotive diesel engine", *Fuel* 87:25-31 (2008).
[10] Song C.L., Zhou Y.C., Huang R.J., Wang Y.Q., Huang Q.F., Lü G., Liu K.M., "Influence of ethanol-diesel blended fuels on diesel exhaust emissions and mutagenic and genotoxic activities of particulate extracts", *Journal of Hazardous Materials* 149:355-363 (2007).
[11] Huang J., Wang Y., Li S., Roskilly A.P., Yu H., Li H., "Experimental investigation on the performance and emissions of a diesel engine fuelled with ethanol-diesel blends", *Applied Thermal Engineering* 29:2484-2490 (2009).
[12] Chen H., Shuai S.J., Wang J.X., "Study on combustion characteristics and PM emission of diesel engines using ester-ethanol-diesel blended fuels", *Proceedings of the Combustion Institute* 31:2981-2989 (2007).
[13] Chotwichien A., Luengnaruemitchai A., Jai-In S., "Utilization of palm oil esters as an additive in ethanol-diesel and butanol-diesel blends", *Fuel* 88:1618-1624 (2009).
[14] Fernando S., Hanna M., "Development of a novel biofuel blend using ethanol-biodiesel-diesel microemulsions: EB-Diesel", *Energy & Fuels* 18:1695-1703 (2004).
[15] Kim H., Choi B., "The effect of biodiesel and bioethanol blended diesel fuel on nanoparticles and exhaust emissions from CRDI diesel engine", *Renewable Energy* 35:157-163 (2010).
[16] Kwanchareon P., Luengnaruemitchai A., Jai-In S., "Solubility of a diesel-biodiesel-ethanol blend, its fuel properties and its emission characteristics from diesel engine", *Fuel* 86:1053-1061 (2007).
[17] Lapuerta M., Armas O., Garcia-Contreras R., "Effect of ethanol on blending stability and diesel engine emissions", *Energy & Fuels* 23:4343-4354 (2009).
[18] Makareviciene V., Sendzikiene E., Janulis P., "Solubility of multi-component biodiesel fuel systems", *Bioresource Technology* 96:611-616 (2005).
[19] Montagne X., "Composition de carburant Diesel à forte teneur en éthanol", Patent FR2895418 (2005).

[20] Pang X., Shi X., Mu Y., He H., Shuai S., Chen H., Li R., "Characteristics of carbonyl compounds emission from a diesel engine using biodiesel-ethanol-diesel as fuel", *Atmospheric Environment* 40:7057-7065 (2006).
[21] Shi X., Pang X., Mu Y., He H., Shuai S., Wang J., Chen H., Li R., "Emission reduction potential of using ethanol-biodiesel-diesel fuel blend on a heavy-duty diesel engine", *Atmospheric Environment* 40:2567-2574 (2006).
[22] Satgé de Caro P., Mouloungui Z., Vaitilingom G., Berge J.C., "Interest of combining an additive with diesel-ethanol blends for use in diesel engines", *Fuel* 80:565-574 (2001).
[23] Pidol L., Lecointe B., Pesant L., Jeuland N., "Ethanol as a diesel base fuel - potential in HCCI mode", *SAE Paper* 2008-01-2506 (2008).
[24] Pidol L., Lecointe B., Jeuland N., "Ethanol as a diesel base fuel: Managing the flash point issue - consequences on engine behavior", *SAE Paper* 2009-01-1807 (2009).
[25] Mzé-Ahmed A., Hadj-Ali K., Diévart P., Dagaut P., "Kinetics of oxidation of a synthetic jet fuel in a jet-stirred reactor: experimental and modeling study", *Energy & Fuels* 24:4904-4911 (2010).
[26] Ramirez H.P., Hadj-Ali K., Diévart P., Dayma G., Togbé C., Moréac G., Dagaut P., "Oxidation of a commercial and surrogate bio-diesel fuels (B30) in a jet-stirred reactor at elevated pressure: experimental and modeling kinetic study", *Proceedings of the Combustion Institute* 33:375-382 (2011).
[27] Dagaut P., Cathonnet M., Rouan J.P., Foulatier R., Quilgars A., Boettner J.C., Gaillard F., James H., "A jet stirred reactor for kinetic studies of homogeneous gas-phase reactions at pressures up to 10 atmospheres", *Journal of Physics E: Scientific Instruments* 19:207-209 (1986).
[28] Kee R.J., Rupley F.M., Miller J.A. "The Chemkin thermodynamic data base", Sandia National Laboratories: Livermore, CA (1987.).
[29] Kee R.J., Rupley F.M., Miller J.A. "CHEMKIN II: a Fortran chemical kinetics package for the analysis of gas-phase chemical kinetics", Sandia National Laboratories: Livermore, CA (1989.).
[30] Glarborg P., Kee R.J., Grcar J.F., Miller J.A. "PSR: a Fortran program for modeling well-stirred reactors", Sandia National Laboratories: Livermore, CA (1986.).
[31] Diévart P., ″Oxydation et combustion en milieu ultra pauvre de carburants types gazoles - étude expérimentale en réacteur agité et modélisation″, PhD thesis, Université de Lille 1 (2008).
[32] Mehl M., Pitz W.J., Sjöberg M., Dec J.E., "Detailed kinetic modeling of low temperature heat release for PRF fuels in an HCCI engine", *SAE Paper* 2009-01-1806 (2009).
[33] Togbé C., May-Carle J.B., Dayma G., Dagaut P., "Chemical kinetic study of the oxidation of a biodiesel-bioethanol surrogate fuel: methyl octanoate-ethanol mixtures", *Journal of Physical Chemistry A* 114:3896-3908 (2010).
[34] Marinov N.M., "A detailed chemical kinetic model for high temperature ethanol oxidation", *International Journal of Chemical Kinetics* 31:183-220 (1999).
[35] Alzueta M.U., Hernandez J.M., "Ethanol oxidation and its interaction with nitric oxide", *Energy & Fuels* 16:166-171 (2002).
[36] Di Y., Cheung C.S., Huang Z., "Comparison of the effect of biodiesel-diesel and ethanol-diesel on the gaseous emission of a direct-injection diesel engine", *Atmospheric Environment* 43:2721-2730 (2009).
[37] He B.Q., Shuai S.J., Wang J.X., He H., "The effect of ethanol blended diesel fuels on emissions from a diesel engine", *Atmospheric Environment* 37:4965-4971 (2003).

[38] Zhang R.D., He H., Shi X.Y., Zhang C.B., He B.Q., Wang J.X., "Preparation and emission characteristics of ethanol-diesel fuel blends", *Journal of Environmental Sciences* 16:793-796 (2004).